

Preparation and Properties of Dopamine Reduced Graphene Oxide and Its Composites of Epoxy

Xinli Hu,¹ Rongrong Qi,¹ Jian Zhu,¹ Jiaqi Lu,¹ Yu Luo,¹ Jieyu Jin,¹ Pingkai Jiang²

¹School of Chemistry and Chemical Engineering, Shanghai Jiao Tong University, Shanghai 200240, China

²Shanghai Key Lab of Electrical Insulation and Thermal Aging, Department of Polymer Science and Engineering, Shanghai Jiao Tong University, Shanghai 200240, China

Correspondence to: R. R. Qi (E-mail: rraqi@sjtu.edu.cn)

ABSTRACT: To improve the thermal and mechanical properties and further to expand its applications of epoxy in electronic packaging, reduced graphene oxide/epoxy composites have been successfully prepared, in which dopamine (DA) was used as reducing agent and modifier for graphene oxide (GO) to avoid the environmentally harmful reducing agents and address the problem of aggregation of graphene in composites. Further studies revealed that DA could effectively eliminate the labile oxygen functionality of GO and generate polydopamine functionalized graphene oxide (PDA-GO) because DA would be oxidated and undergo the rearrangement and intermolecular cross-linking reaction to produce polydopamine (PDA), which would improve the interfacial adhesion between GO and epoxy, and further be beneficial for the homogenous dispersion of GO in epoxy matrix. The effect of PDA-GO on the thermal and mechanical properties of PDA-GO/epoxy composites was also investigated, and the incorporation of PDA-GO could increase the thermal conductivity, storage modulus, glass transition (T_g), and dielectric constant of epoxy. © 2013 Wiley Periodicals, Inc. *J. Appl. Polym. Sci.* 2014, 131, 39754.

KEYWORDS: composites; conducting polymers; properties and characterization; thermal properties; resins

Received 20 January 2013; accepted 14 July 2013

DOI: 10.1002/app.39754

INTRODUCTION

In past years, epoxy molding compounds have been extensively used in electronic packaging due to its exceptional weather and chemical resistance, excellent mechanical and electric properties.¹ And the heat dissipation is an important topic with the rapid development of electronic devices heading for miniaturization, because it directly affects the lifespan of high-performance electronic devices.^{2,3} However, the poor thermal conductivity of pure epoxy (0.260 W/m K) makes it difficult to remove immediately and guarantee the stability of electronic devices.⁴ To address this problem, a variety of fillers, e.g., Al_2O_3 ,⁵ AlN ,⁶ BN ,⁷ and Cu powder,⁸ have been employed to improve polymer matrix' thermal conductivity. Nevertheless, a large amount of fillers are necessary to achieve the requirement of thermal conductivity, which may result in deterioration of mechanical and processing properties of epoxy matrix.⁹ Recently, carbon-based materials, including carbon black, graphite, carbon nanotubes as well as graphene, have been employed as fillers to enhance the thermal conductivity of polymers. Among all the carbon-based materials, graphene has attracted

extensive attention due to its ultrahigh mechanical property, excellent electrical and thermal conductivity, exceptional optical property, and abundant resources (graphite) in recent years.^{10–15} The prominent performances of graphene have made it an ideal material for applications in the field of optoelectronic and microelectronic devices.^{16–18} In the past few years, a variety of methods including chemical conversion, electrochemical reduction and thermal exfoliation have been developed to obtain graphene.^{19–22} Among these reported methods, the chemical reduction is one of the most common methods to prepare graphene because of its high efficiency and bulk productivity.¹⁹ However, the commonly used reducing reagents (e.g., hydrazine, dimethylhydrazine, and NaBH_4) are harmful to environment,^{23–25} and the resulted graphene has a strong tendency to restack owing to the π - π interactions.²⁶ On the other hand, the poor dispersion of graphene in matrix also restricted its applications due to incompatibility of inorganic fillers and organic polymer matrix. Thus, it is desirable to choose a green nontoxic reducing reagent which can both reduce and functionalize GO preventing the aggregation of the reduced GO. Taking

into account epoxy matrix, the reducing reagent shall bear some reactive groups after the reduction of GO, which can further react with matrix and therefore enhance the interfacial adhesion between reduced GO and epoxy matrix.

Dopamine (DA), a simple nontoxic organic chemical in the catecholamine family, is produced from the brains of many organisms including human, and it consists of an amine group linked to a catechol structure and plays a critical role in the function of the central nervous system.^{27,28} In past years, dopamine was also employed as reducing agent with oxidation of catechol groups to the quinone form.^{29,30} Recently, Izabela et al. successfully used dopamine derivatives to reduce and non-covalently functionalize graphene oxide,³¹ implying that dopamine or its derivatives are good reducing reagents. On the other hand, the remaining amine after oxidation of dopamine can react with epoxy group when dopamine has been used as reducing agent, which could prevent the agglomeration of graphene into graphitic structures and further improve the interfacial adhesion between graphene and epoxy. Thus, it is promising to utilize DA to reduce GO and then incorporate into epoxy matrix as enhancing materials, because of the advantages of DA including nontoxic property, restraining agglomeration, and amino functionalization of DA-GO.

In this study, to expand the applications of epoxy and graphene materials, especially in the field where thermal properties is required, an effective approach is developed to prepare epoxy composites containing DA reduced GO, in which GO was reduced by DA first, then PDA-GO/epoxy composites were obtained. The obtained PDA-GO and PDA-GO/epoxy composites were characterized well. Furthermore, the effect of PDA-GO on the thermal and mechanical properties of PDA-GO/epoxy composites was also investigated, and the incorporation of PDA-GO could increase the thermal conductivity, storage modulus, and glass transition (T_g) of epoxy.

EXPERIMENTAL

Materials

Natural graphite powder, sulfuric acid (H_2SO_4), hydrochloric acid (HCl), potassium persulfate ($K_2S_2O_8$), phosphorus pentoxide (P_2O_5), potassium permanganate ($KMnO_4$), disodium hydrogen phosphate dodecahydrate ($Na_2HPO_4 \cdot 12H_2O$), and sodium dihydrogen phosphate dihydrate ($NaH_2PO_4 \cdot 2H_2O$) were purchased from Sinopharm Chemical Reagent Co., Shanghai, China. Hydrogen peroxide (H_2O_2) was obtained from Shanghai Lingfeng Chemical Reagent Co., Shanghai, China. Diglycidyl ether of bisphenol A epoxy (618), curing agent methyl tetrahydrophthalic anhydride (MTHPA) and accelerator 2,4,6-tris(dimethylaminomethyl) phenol (TAP) were supplied by Shanghai Resin Factory, Co., Shanghai, China. Dopamine hydrochloride was supplied by Sigma-Aldrich Co., Milwaukee, Wisconsin. All reagents were used as received.

Synthesis of Graphene Oxide

GO was synthesized from natural graphite according to a modified Hummers method.³² Graphite powder (4.0 g) was dispersed firstly in the solution of concentrated sulfuric acid (30 mL), potassium persulfate (6.0 g), and phosphorus pentoxide (6.0 g),

Table I. Formulation of Dopamine Reduced Graphene Oxide/Epoxy Composites

Components	Compounds	Content (phr)
Matrix	Diglycidyl ether of bisphenol A epoxy (618)	100
Curing agent	Methyl tetrahydrophthalic anhydride (MTHPA)	85
Accelerator	2,4,6-Tris(dimethylaminomethyl) phenol (TAP)	0.4
Filler	Dopamine reduced graphene oxide (PDA-GO)	Variant

then the solution was heated to 80°C and kept stirring for 6 h in oil-bath. After that, the mixture was cooled to room temperature and diluted with deionized water (2 L) overnight, and then products were obtained by filtering and dried at 60°C for 24 h. The pre-oxidized graphite was further oxidized following: The pretreated graphite powder was put into concentrated sulfuric acid (300 mL) at 0°C, and potassium permanganate (35 g) was added under stirring and cooling conditions in ice-bath. Then the mixture was kept at 35°C overnight and diluted with deionized water (2 L) followed by adding 30% hydrogen peroxide (100 mL) drop-by-drop. The mixture was filtered and washed with 1 : 10 hydrochloric acid aqueous solution (2 L) and deionized water (1 L) to remove the metal ions and acid. Then the resulted graphene oxide was dried at 80°C in vacuum oven for 24 h.

Reduction of Graphene Oxide with Dopamine (PDA-GO)

Dopamine hydrochloride (0.1 g) was dispersed in 300 mL of phosphate buffer solution (pH = 8.5) through an ultrasonic process. Then 0.2 g of as-prepared graphene oxide was added to a round bottom flask, and the reduction was carried out by stirring at 60°C for 24 h. After that, the reaction solution was washed with deionized water repeatedly to remove the residual dopamine, until the solution was neutral. Finally, black PDA modified graphene (PDA-GO) was obtained by filtering and dried overnight.

Preparation of PDA-GO/Epoxy Composites

Epoxy resin was firstly blended with curing agent, accelerator and PDA-GO, according to the designed mass-fraction ratio (Table I), and homogenous mixture was obtained after being stirred by magnetic stirring for 1 h at room temperature and 300 rpm/min. Then the mixture was degassed for about 20 min to remove bubbles at 80°C in an oven. After that, the liquid mixture was transferred to a plate mold, and the curing condition was set as 100°C for 4 h and 150°C for 2 h under a pressure of around 10 MPa. Afterwards, the cured sample was left to cool down slowly to room temperature. Thus, epoxy-based composites with PDA-GO loadings ranging from 0 to 15 phr were prepared.

Characterization

Fourier transform infrared spectroscopy (FT-IR) was performed over the wave number range of 4000–500 cm^{-1} on a Spectrum

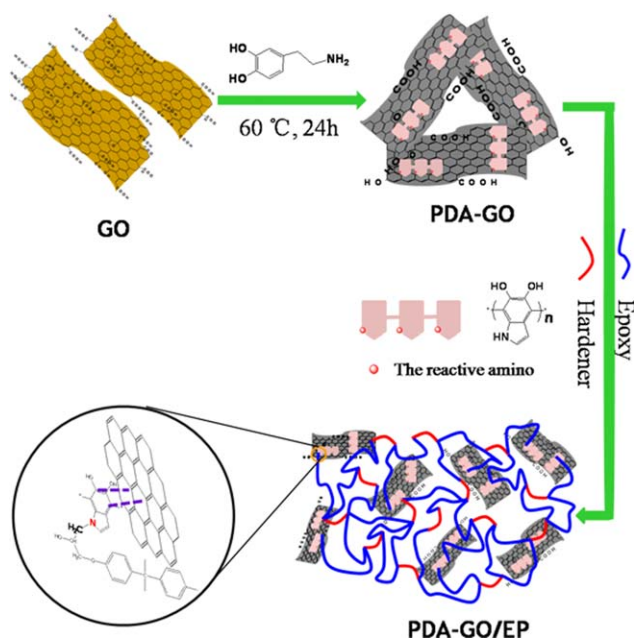


Figure 1. The schematic diagram of PDA-GO/epoxy composites. [Color figure can be viewed in the online issue, which is available at wileyonlinelibrary.com.]

100 spectrometer (Perkin Elmer, Waltham, MA). X-ray diffraction (XRD) was conducted at room temperature on a D/max-2200/PC diffractometer (Japan Rigaku Corporation, Tokyo, Japan) at a scan rate $4^{\circ}/\text{min}$. Raman spectra of pure graphite, GO, and PDA-GO were obtained on a inVia-reflex (Renishaw, Gloucestershire, UK). Ultraviolet spectra were carried out on Lambda 750S spectrometer (Perkin Elmer, Waltham, MA). X-ray photoelectron spectra (XPS) were carried out on a PHI VersaProbe 5000 Auger electron spectrometer (Philips Electronics, Amsterdam, Holland). Thermogravimetric analysis (TGA) was conducted on a Q5000IR (TA Instruments, New castle, Delaware) at a heating rate of $20^{\circ}\text{C}/\text{min}$ from room temperature to 700°C under nitrogen atmosphere. Transmission electron microscope (TEM) was carried out on a JEM-2100F (JEOL, Tokyo, Japan) electron microscope at an acceleration voltage of 200 KV. The specimen of PDA-GO/epoxy composites for TEM observation were prepared by placing one drop of uncured PDA-GO/epoxy on the top surface of deionized water to form one ultrathin film, followed by immersing lacey coated copper grids in the water and got out. Afterwards, the copper grids with PDA-GO/epoxy were placed in an oven for curing at 100°C for 4 h and 150°C for 2 h. The samples have also been observed by TEM using the ultrathin section of the curing sample. Morphological analysis was carried out on frozen fractured samples, and the corresponding cross sections were examined by field emission scanning electron microscope (FESEM; JSM-7401F, JEOL, Akishima, Japan). The surface of samples was dried under vacuum and then coated with a conductive gold layer before FESEM analysis. Differential scanning calorimetry measurements were performed on a Q2000 MDSC (TA Instruments, New castle, Delaware) with samples of about 4 mg sealed in aluminum pans under nitrogen atmosphere. The samples were heated at a rate of $20^{\circ}\text{C}/\text{min}$ from 40 to 280°C . Thermal

conductivity was measured on disk samples by laser flash method (LFA447 NanoFlash, NETZSCH Ltd, Hanau, Germany). Specimens with dimension of 1 mm in thickness and 12.7 mm in diameter were cut from the core region of compression-molded sheets. The surfaces of specimens were coated with a layer of carbon before determining the thermal conductivity. Dynamic mechanical measurements (DMA) were carried out in tension mode by employing a DMA Q800 (TA Instruments, New castle, Delaware) dynamic mechanical viscoelastometer. The temperature rising rates were at $2^{\circ}\text{C}/\text{min}$ from 30 to 200°C , and the test frequency was 1Hz. The dielectric properties of all the samples were measured by a CONCEPT 40 brand frequency impedance analyzer (Novocontrol Company, Hundsangen, Germany) in the frequency range of 1 to 10^6 Hz and at room temperature. The working electrodes were prepared by depositing gold films on both sides of the samples. Sample size is $6 \times 6 \times 1$ mm.

RESULTS AND DISCUSSION

In terms of polymer composites with graphene, the poor dispersion of graphene in matrix has restricted its wide applications due to incompatibility between inorganic fillers and organic polymer matrices. To address this problem, dopamine is used to reduce graphene oxide as phenolic hydroxyl of dopamine possessing water solubility and oxidation resistance. Upon reaction, dopamine is oxidated and self-polymerized into polydopamine (PDA-GO). At the same time, the aromatic structure and amino group of PDA-GO can form the π - π stacking with reduced graphene oxide and react with epoxy matrix, respectively (as shown in Figure 1), which could further prevent the agglomeration of graphene and improve interfacial adhesion between graphene and epoxy. And then homogeneous composites of PDA-GO/epoxy can be obtained. In this study, graphene oxide is first prepared by modified Hummers method, and then it is reduced and functionalized by dopamine to form reduced graphene oxide (PDA-GO), and finally PDA-GO/epoxy composites are obtained.

Characterization of PDA-GO

To examine whether DA can reduce GO, FT-IR spectra of DA, pure GO and PDA-GO are shown in Figure 2. The corresponding peaks for C—O stretching vibration at 1096 cm^{-1} , OH deformation vibration at 1390 cm^{-1} , and C—O (alkoxy) stretching vibration at 1040 cm^{-1} in the spectrum of GO disappear in the spectrum of PDA-GO, implying the removal of oxygen functionalities from PDA-GO. Furthermore, the significant change of C=O stretching vibration peak at 1625 cm^{-1} in PDA-GO also indicates the reduction of GO to graphene. On the other hand, the new peaks (in the spectrum of PDA-GO) at 1228 and 1972 cm^{-1} caused by C—N stretching vibration indicate that the C—N group is bonded to graphite planar surface during the reduction process and PDA-GO is functionalized by amino groups. Moreover, compared with DA and GO, the peak intensity of OH stretching vibration of PDA-GO at 3420 cm^{-1} decreases significantly, also implying that the partial elimination of OH functionalities. Based on the above analysis, one can conclude that GO is both reduced and functionalized by DA.

From XRD patterns (Figure 3), one can see that pristine graphite exhibits a typical (002) peak at 26.46° corresponding to the

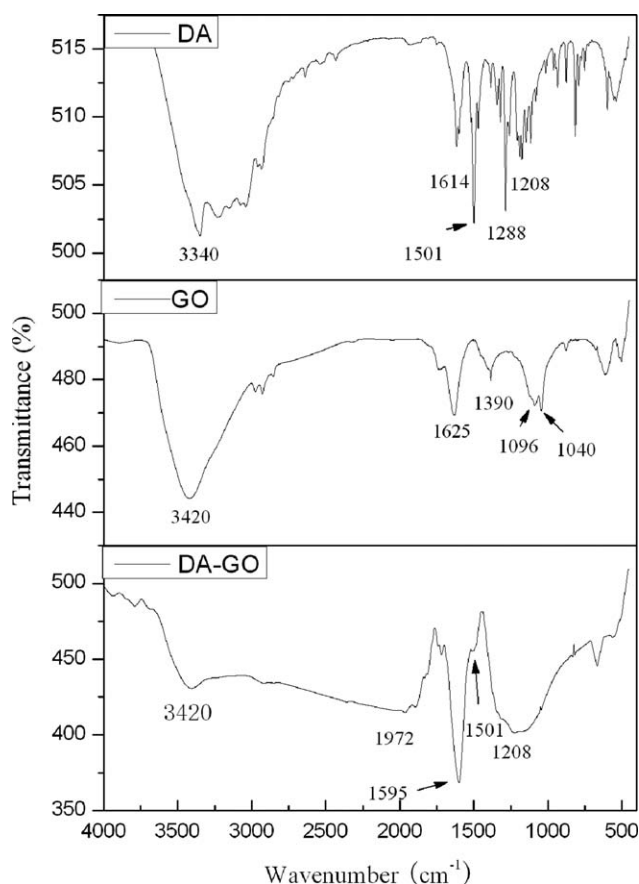


Figure 2. FT-IR spectra of DA, pure GO and PDA-GO.

(002) inter-planar spacing of 0.346 nm, and the 002 peak shifts to 9.24° (0.959 nm) after graphite has been oxidized to GO, meaning the formation of oxygen-containing functional groups on graphite surface.^{33,34} Upon reduction, the obtained GO is reduced by dopamine, the peak of GO at 9.24° disappears, implying the removal of oxidized functional groups from the interlayer of GO, and the exfoliation of PDA-GO.

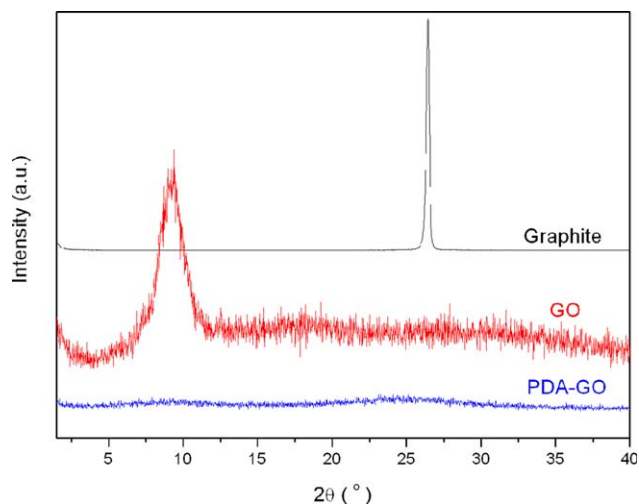


Figure 3. XRD patterns of graphite, GO and PDA-GO. [Color figure can be viewed in the online issue, which is available at wileyonlinelibrary.com.]

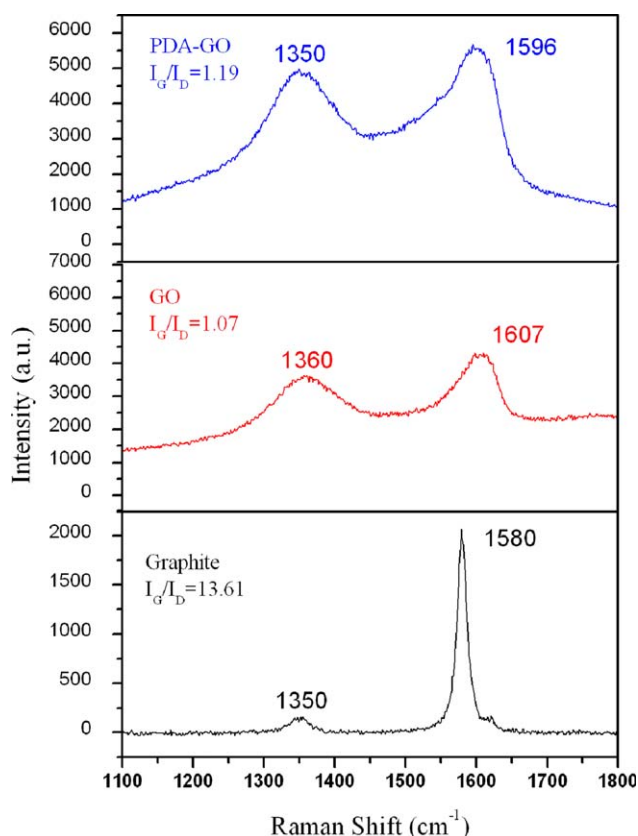


Figure 4. Raman spectra of graphite, GO, and PDA-GO. [Color figure can be viewed in the online issue, which is available at wileyonlinelibrary.com.]

To further verify the reduction of GO, Raman spectra of graphite, GO and DA-GO are shown in Figure 4. All of them have two bands at around 1580 and 1350 cm^{-1} , corresponding to G band (first-order scattering of E_{2g} phonons by sp^2 carbon atoms) and D band (defects inherent in the graphite and the edge effect of graphite, A_{1g} mode), respectively.³⁵ Compared to pristine graphite, the G band and D band of GO shift to higher position at 1607 and 1360 cm^{-1} , the intensity of D band becomes higher, and the intensity ratio of D band to G band (I_D/I_G) of pristine graphite changes from 13.61 to 1.07 of GO, implying the destruction of sp^2 character upon oxidation. However, the G and D band of PDA-GO shift to lower region when GO is reduced by DA, and the I_D/I_G changes to 1.19, implying some restore of graphene structure, which is due to the removal of oxygen functionalization and restoration of the sp^2 structure after the reduction reaction.³⁶ The above results also indicate that GO can be reduced by DA, and PDA modified GO can be obtained.

As shown the UV-vis absorption spectra of GO and PDA-GO (Figure 5), the peak at 228 nm of GO corresponds to $\pi-\pi^*$ electronic transition of C=C from the highest occupied molecular orbital (HOMO) to the lowest unoccupied molecular orbital (LUMO), whereas the characteristic peak at 300 nm is attributed to $n-\pi^*$ transition of C=O bonding. After being reduced by dopamine, the characteristic peak at 228 nm remains unchanged, while the peak at 300 nm disappears, also implying

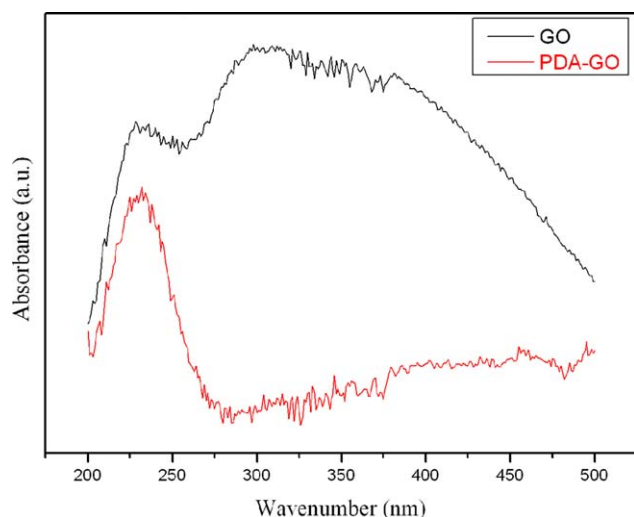


Figure 5. UV-vis spectra of GO and PDA-GO. [Color figure can be viewed in the online issue, which is available at wileyonlinelibrary.com.]

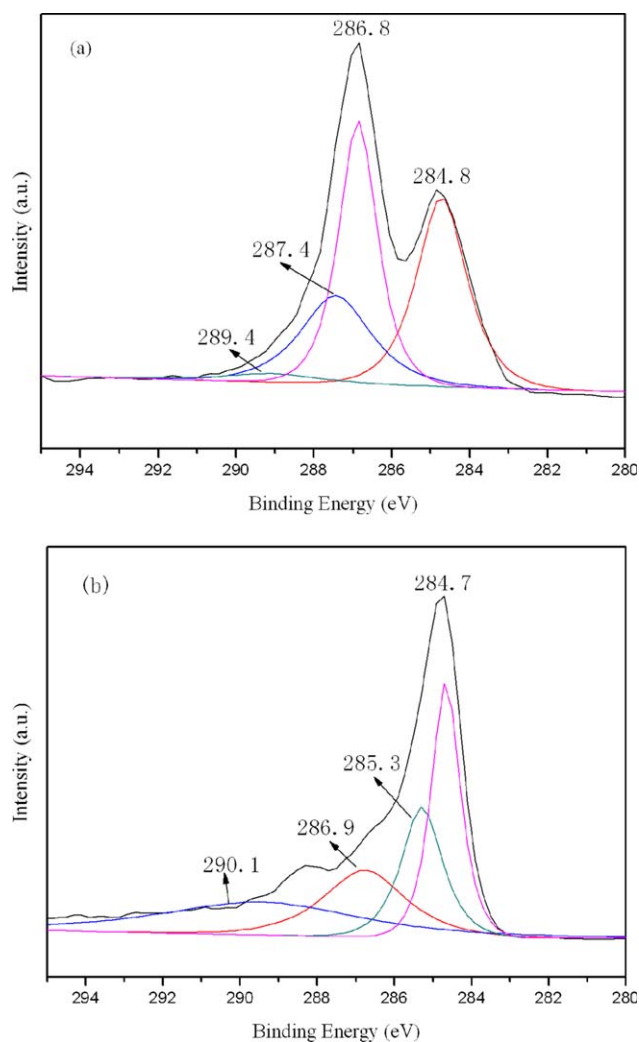


Figure 6. XPS spectra of C1s region of (a) GO and (b) PDA-GO. [Color figure can be viewed in the online issue, which is available at wileyonlinelibrary.com.]

Table II. Elemental Composition of GO and PDA-GO Determined by XPS

Samples	Carbon (atomic percentage %)	Nitrogen (atomic percentage %)	Oxygen (atomic percentage %)
GO	36.69	0	63.31
PDA-GO	45.80	7.46	46.74

GO nanosheets have been reduced and the aromatic structure within the GO nanosheets is restored.³⁷

Chemical compositions of GO and PDA-GO were tested by XPS spectrum. From the C1s core level spectra of GO [Figure 6 (a)], one can see that the C1s signal of GO can be decomposed into four components: C=C (284.8 eV), C-OH (286.8 eV), C-O-C (287.4 eV), and C=O (289 eV), respectively.^{38,39} After being reduced by dopamine, the intensity of DA-GO spectrum decreases and the main peaks shift because of the change of chemical environments and subsequently elimination of oxygen functionalities [Figure 6(b)]. From Table II, one can see that the ratio of C to O of PDA-GO remarkable increases in comparison to that of GO. However, compared with the reported data of C/O ratio (2.3) of GO,⁴⁰ the ratio of C/O (0.58) of GO we prepared is much lower, which may be due to the higher oxidation of GO.

The TGA plots of graphite GO and PDA-GO is shown in Figure 7. The TGA pattern of graphite shows almost no mass loss owing to its perfect two-dimensional structure.³⁸ Two degradation steps are displayed for GO curve. The first degradation step initiates at 138°C, stemming from the loss of oxygen functional groups. The second step degradation starts at 211°C due to the pyrolysis of ring carbon.⁴¹ However, the PDA-GO starts to oxidize at a higher temperature around 145°C. In addition, compared with 56 wt % weight loss at 700°C experienced by pure GO, PDA-GO undergoes 34 wt %. This data may be due to the fact that GO bears a larger amount of oxygen-containing groups; while PDA-GO possess less functional groups after reduction, suggesting graphitic structure of PDA-GO has restored.

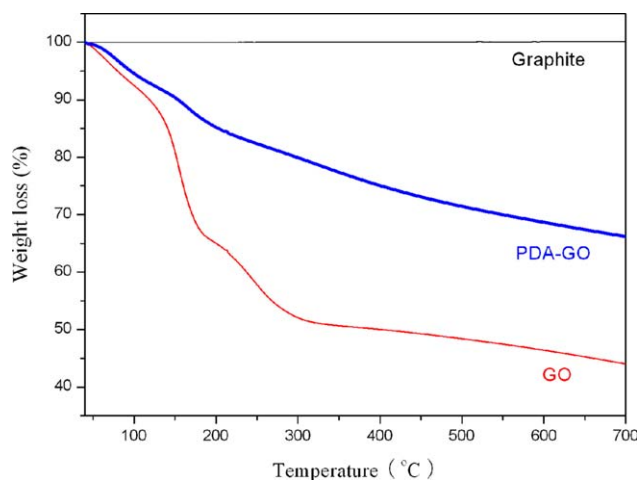


Figure 7. TGA plots of graphite, pure GO and PDA-GO. [Color figure can be viewed in the online issue, which is available at wileyonlinelibrary.com.]

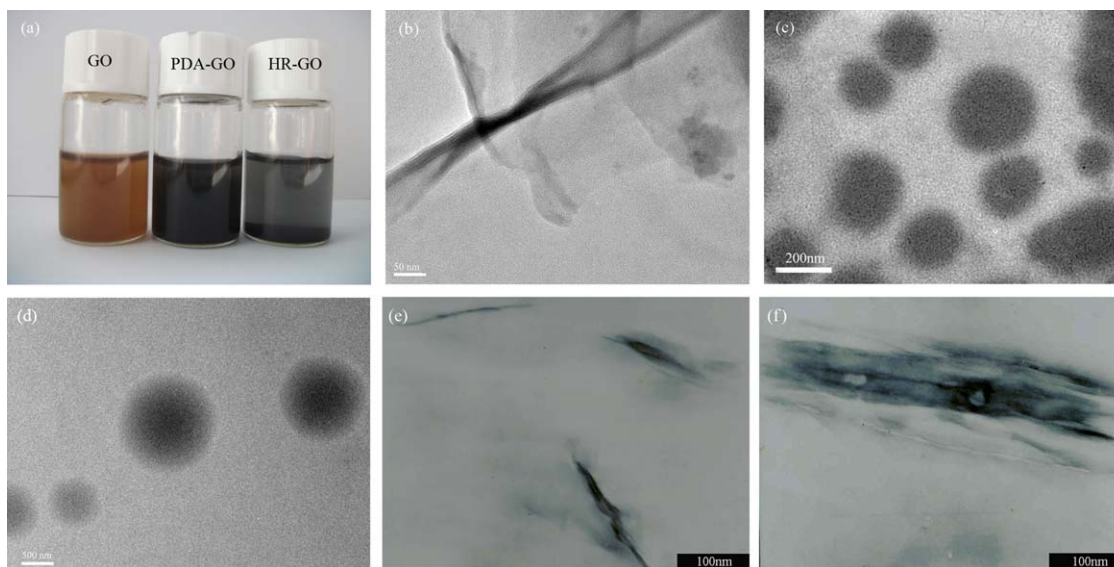


Figure 8. Digital photographs of (a) GO, PDA-GO, and HR-GO. TEM image of (b) PDA-GO, (c) 1 phr PDA-GO/epoxy composite, and (d) 1 phr HR-GO/epoxy composite using the sample curing on the copper grid, (e) 1 phr PDA-GO/epoxy composite and (f) 1 phr HR-GO /epoxy composite using the ultrathin section of the curing sample. [Color figure can be viewed in the online issue, which is available at wileyonlinelibrary.com.]

The above characterizations, in terms of FT-IR, XRD, UV-vis, XPS, and TGA, indicate that GO has been reduced and functionalized by DA, which paves the way for the preparation of PDA-GO/epoxy composites.

Characterization and Properties of PDA-GO/Epox Composites

PDA-GO/epoxy composites were prepared by incorporating the as-prepared PDA-GO into epoxy resins, and the effect of PDA-GO content on the microstructure, curing reaction of epoxy resin and properties of PDA-GO/epoxy composites has been studied, such as mechanical properties and thermal conductivity.

Microstructure of PDA-GO/Epox Composites. The as-synthesized GO is a kind of black powder, while its aqueous solution is in

light brown color. Upon reaction with DA, the PDA-GO is readily dispersed in water and appears dark color, as shown in Figure 8(a). This kind of color change also can be considered as a witness for chemical reduction of graphene oxide sheets because of the partial restoration of the π network within the carbon structure^{42,43} However, the hydrazine reduction of GO (HR-GO) can not readily dispersed in water and only form a precipitate, which also implying the successful functionalization of PDA-GO. The transparent sheets appeared in Figure 8(b) indicate the complete exfoliation of PDA-GO. Furthermore, PDA-GO nanoplatelets with the average size approximately 200 nm can be homogeneously dispersed in epoxy resins, and no large agglomerates are observed in Figure 8(c,e). However, HR-GO is heterogeneously dispersed in HR-GO/epoxy composite, and the size (500 nm to 1 μm) is larger than that of PDA-GO in Figure 8(d,f), and some agglomerates can be observed. And, it is observed PDA-GO exhibit good adhesion to neat epoxy. In contrast, the size of HR-GO is larger and could not be dispersed uniformly in epoxy matrix.

The good dispersion of PDA-GO within epoxy matrix can be attributed to the functional groups on the PDA-GO, in which the amino functionalities of PDA-GO can react with epoxy functional groups in epoxy to form chemical bonds, enhancing the interaction between PDA-GO and epoxy matrix, and further facilitating PDA-GO dispersing in the epoxy matrix.

Curing Reaction of PDA-GO/Epox Composites. To investigate the effect of PDA-GO on the curing reaction of epoxy resin, DSC of epoxy resin and PDA-GO/epoxy composite has been carried (Figure 9). It is evident that the exothermal peak of PDA-GO/epoxy composite shifts to lower temperature (155.6 $^{\circ}\text{C}$) compared to the exothermal peak temperature (165.5 $^{\circ}\text{C}$) of pure epoxy resin, suggesting that PDA-GO would act as a catalyst to accelerate the curing process of epoxy resin. Furthermore, the enthalpy of PDA-GO/epoxy composite increases from 208.3 J/g of pure

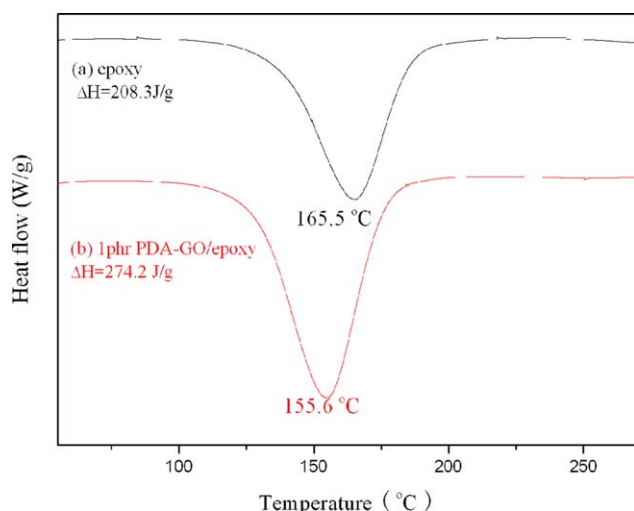


Figure 9. DSC curves of (a) epoxy resin, (b) 1 phr PDA-GO/epoxy composites. [Color figure can be viewed in the online issue, which is available at wileyonlinelibrary.com.]

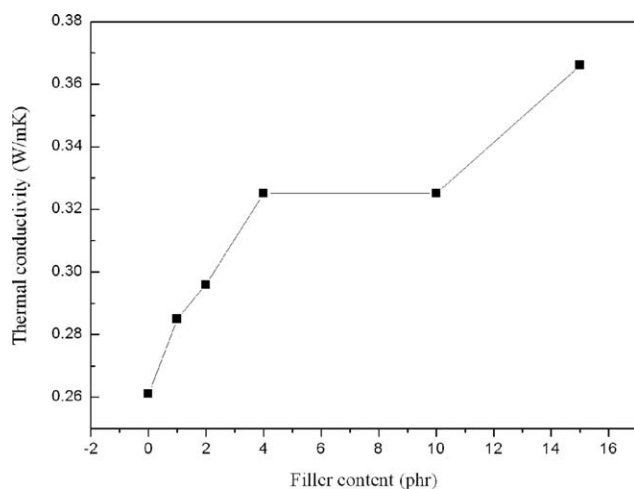


Figure 10. Effect of PDA-GO on the thermal conductivity of epoxy composites.

epoxy to 274.2 J/g for 1 phr PDA-GO/epoxy composite. The above results also indicate the chemical cross-linking reaction between amino of PDA-GO and epoxy matrix, and increase of epoxide contents in composites, which also confirms the enhanced interfacial interaction between PDA-GO and epoxy matrix. Similar phenomenon also has been reported in other system.⁴⁴

Thermal Conductivity PDA-GO/Epoxly Composites. Because of the excellent thermal conductivity of graphene, it is expected to improve the thermal conductivity of epoxy by incorporating graphene. In general, the thermal conductivity of composites is affected by graphene structure, loading, dispersion, and the thermal resistance of interface between graphene and epoxy matrix. From the dependence of the thermal conductivity of epoxy composites on PDA-GO content (Figure 10), one can see that the thermal conductivity of PDA-GO/epoxy composites increases considerably along with the increase of PDA-GO. Thermal conductivity of 4 phr PDA-GO/epoxy composites increases about 25.4%, compared with that of pure epoxy resin. When PDA-GO loading is lower than 4 phr, the thermal conductivity is low, indicating that PDA-GO nanoplatelets are isolated by polymer matrix. After that, when the PDA-GO loading reaches the percolation threshold of PDA-GO/epoxy composites, the thermal conductivity increases slowly. It is noticeable that the thermal conductivity of composites reaches to 0.37 W/mK when the amount of PDA-GO is 15 phr, increasing about 40% more than that of pure epoxy resin. Evidently, the addition of PDA-GO could contribute to increase of thermal conductivity of epoxy based composites. The fact also implies that the amine group on the PDA-GO will react with epoxy and enhance the interfacial adhesion between GO and epoxy. On the other hand, the reducibility of PDA is relatively weak, so the un-complete reduction of GO (as shown in XPS) may be obtained, which leads to thermal conductivity is lower than that of Ref. 22.

Mechanical Properties of PDA-GO/Epoxly Composites. Overall, incorporation of fillers regardless of Al_2O_3 , PDA-GO will increase the mechanic properties such as storage modulus and T_g . However, the mechanical properties variation is monotonic for conventional filler like Al_2O_3 ,⁴⁵ while the effect of PDA-GO

on mechanical properties is not monotonic. This may result from both the effect of extent of exfoliation and interaction between PDA-GO and epoxy.⁴⁶ Figure 11(a) shows the storage modulus of pure epoxy resin and epoxy composites containing varying PDA-GO content as a function of temperature at 1 Hz. The storage modulus of composites increases with the increase of PDA-GO, and reaches to maximum when PDA-GO content is 15 phr, which may be attributed to the exceptional modulus of graphene.⁴⁷ The above results indicate that the mechanical performance of PDA-GO/epoxy composite is strengthened with the addition of PDA-GO. From the $\tan \delta$ of pure epoxy and PDA-GO/epoxy composites with different PDA-GO content at 1 Hz [Figure 11(b)], one can see that the T_g of composites shifts toward the high-temperature region with the increase of PDA-GO loading, indicating that the interfacial action between PDA-GO and epoxy matrix can increase the degree of cross linking and constraint the mobility of the chain segment. But the T_g variation of the composites is not monotonic. This may result from the effect of extent of exfoliation, interaction between PDA-GO and epoxy and agglomeration. First, the extent of exfoliation prevents the epoxy molecular chain from movement

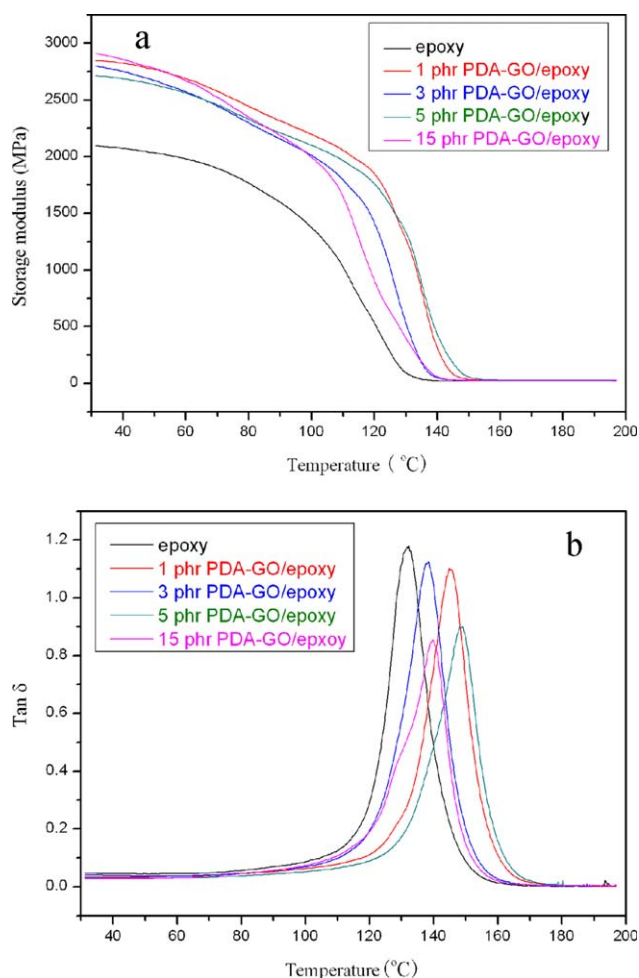


Figure 11. (a) Storage modulus and (b) $\tan \delta$ of pure epoxy and PDA-GO/epoxy composites with different PDA-GO contents at 1 Hz. [Color figure can be viewed in the online issue, which is available at wileyonlinelibrary.com.]

which results in the increase of T_g . Second, due to the interaction between PDA-GO and epoxy, the PDA-GO partly takes place of curing agent, which decreases crosslinking degree accordingly leading to the reduction of T_g eventually. Third, for more PDA-GO composites, PDA-GO may form some small, aggregated, filler cluster structures, thus the T_g decreases as a result of the appearance of voids. The above-mentioned factors make the T_g variation in not monotonic. However, the T_g of all the composites is higher than that of pure epoxy. The summary of T_g data of PDA-GO/epoxy composites is shown in Table III.

Dielectric Properties of PDA-GO/Epoxy Composites. Figure 12 gives the frequency dependent dielectric parameters for the PDA-GO/epoxy composite. The dielectric constant and dissipation factors of the PDA-GO/epoxy composite have relatively weak frequency dependence. For instance, the 100 Hz dielectric constant of PDA-GO/epoxy composite with a slight increase from 6.87 to 7.64 [Figure 12(a)], while the dissipation factors still less than 0.015 [Figure 12(b)], indicating that it is still a promising graphene-based dielectric composites.

The increase of dielectric constant in PDA-GO composites can be explained as follows using micro-capacitor model^{48,49}: In the nanocomposites, epoxy resin is electrically insulated, while PDA-GO is conductive. For the percolative composites, PDA-GO nanoplatelets are isolated by polymer matrix as a thin dielectric layer, which is identical to the case where a large number of nanocapacitors are connected with each other. PDA-GO acts as electrodes and the thin layer of epoxy between them can be considered as dielectric. These PDA-GO and epoxy form abundant micro-capacitor. When the ratio of PDA-GO increases, the number of micro-capacitor increases while the thickness of dielectric layer decreases, which results in high dielectric constant. Meanwhile, there are isolated PDA-GO in epoxy matrix, which hinders the PDA-GO nanoplatelets directly connecting to each other, and the dielectric loss increases. On the other hand, dispersion of PDA-GO in epoxy matrix is an essential factor which has influence on the dielectric constant. Good dispersity of PDA-GO, as show in TEM images, lead to higher dielectric constant and lower dielectric loss. As a result, both the dielectric constant and dielectric loss of PDA-GO/epoxy are higher compared with neat epoxy.^{50,51}

CONCLUSIONS

In this study, DA functionalized reduced GO has successfully been prepared firstly, and then homogeneously PDA-GO/epoxy composites with good thermal and mechanical properties have been prepared by incorporating dopamine reduced graphene oxide (PDA-GO) into epoxy matrix because the reactive amine functionality of PDA-GO is beneficial for them dispersing in epoxy matrix. Further studies reveal that the exothermal peak of 1 phr PDA-GO/epoxy composite shifts to lower temperature

Table III. Summary of T_g Results of for PDA-GO Composites Determined by DMA

PDA-GO content (phr)	0	1	3	5	15
T_g (°C)	131.9	145.4	138.2	148.7	140.1

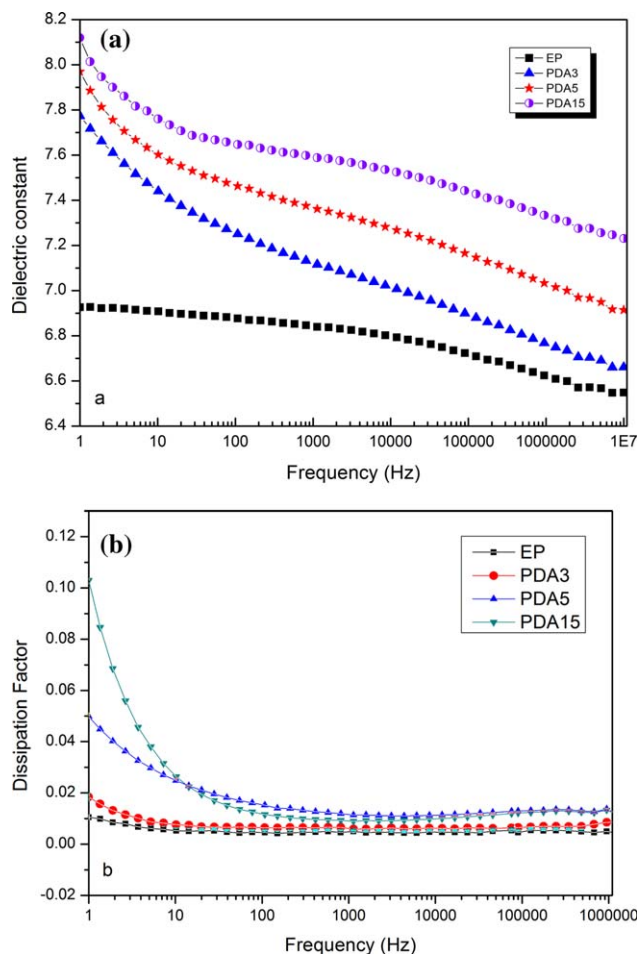


Figure 12. Dielectric properties of PDA-GO/epoxy composites as a function of PDA-GO content: (a) Dielectric constant and (b) dissipation factor. [Color figure can be viewed in the online issue, which is available at wileyonlinelibrary.com.]

(from 165.5°C for pure epoxy to 155.6°C for 1 phr PDA-GO/epoxy), indicating that PDA-GO would act as a catalyst to accelerate the curing reaction. In additions, the enthalpy (274.2 J/g) during curing reaction is larger than that of pure epoxy (208.3 J/g); also implying that the increase of reactive sites of functionalized PDA-GO would form a chemical linkage with epoxy matrix during crosslinking reaction. The thermal conductivity of 15 phr PDA-GO/epoxy composites increases 40% in comparison to that of pure epoxy resin, the storage modulus, T_g and the dielectric constant of PDA-GO/epoxy composites also increase with the addition of PDA-GO.

ACKNOWLEDGMENTS

The work described in this article was supported by the National Science Foundation of China (No: 21173145 and 51133003), Shanghai nano special project (12nm0503502) and Shanghai Leading Academic Discipline Project (No. B202).

REFERENCES

- Hirao, K.; Watari, K.; Hayashi, H.; Kitayama, M. *MRS Bull.* **2001**, *26*, 451.

2. Zhou, W. Y.; Qi, S. H.; Tu, C. C.; Zhao, H. Z. *J. Appl. Polym. Sci.* **2007**, *104*, 2478.
3. Ruth, R.; Donaldson, K. Y.; Hasselman, D. P. H. *J. Am. Ceram. Soc.* **1992**, *75*, 2887.
4. Garrett, K. W.; Rosenberg, H. M. *J. Phys. D: Appl. Phys.* **1974**, *7*, 1247.
5. An, K. H.; Park, S. J. *Bull. Korean Chem. Soc.* **2012**, *33*, 3258.
6. Teng, C. C.; Ma, C. C. M.; Chiou, K. C.; Lee, T. M. *Compos.: Part B* **2012**, *43*, 265.
7. Wattanakul, K.; Manuspiya, H.; Yanumet, N. J. *Appl. Polym. Sci.* **2011**, *119*, 3234.
8. Im, H.; Kim, J. *Polym. Composite* **2010**, *31*, 1669.
9. Zhou, W. Y.; Wang, C. F.; Ai, T.; Wu, K.; Zhao, F. J.; Gu, H. Z. *Compos.: Part A* **2009**, *40*, 830.
10. Im, H.; Kim, J. *Carbon* **2012**, *50*, 5429.
11. Fang, M.; Long, J.; Zhao, W. W.; Wang, L. W.; Chen, G. H. *Langmuir* **2010**, *26*, 16771.
12. Balandin, A. A.; Ghosh, S.; Bao, W. Z.; Calizo, I.; Teweldebrhan, D.; Miao, F.; Lau, C. N. *Nano Lett.* **2008**, *8*, 902.
13. Wang, S. J.; Geng, Y.; Zheng, Q.; Kim, J. K. *Carbon* **2010**, *48*, 1815.
14. Nair, R. R.; Blake, P.; Grigorenko, A. N.; Novoselov, K. S.; Booth, T. J.; Stauber, T.; Peres, N. M. R.; Geim, A. K. *Science* **2008**, *320*, 1308.
15. Im, H.; Kim, J. *Carbon* **2012**, *50*, 5429.
16. Zhang, X. Q.; Feng, Y. Y.; Tang, S. D.; Feng, W. *Carbon* **2010**, *48*, 211.
17. Schedin, F.; Geim, A. K.; Morozov, S. V.; Hill, E. W.; Blake, P.; Katsnelson, M. I.; Novoselov, K. S. *Nat. Mater.* **2007**, *6*, 652.
18. Zhang, W. L.; Liu, Y. D.; Choi, H. J. *Carbon* **2012**, *50*, 290.
19. Zhang, T.; Zhang, D.; Shen, M. *Mater. Lett.* **2009**, *63*, 2051.
20. Lee, K. R.; Lee, K. U.; Lee, J. W.; Ahn, B. T.; Woo, S. I. *Electrochem. Commun.* **2010**, *12*, 1052.
21. Ju, H. M.; Huh, S. H.; Choi, S. H.; Lee, H. L. *Mater. Lett.* **2010**, *64*, 357.
22. Teng, C. C.; Ma, C. C. M.; Lu, C. H.; Yang, S. Y.; Lee, S. H.; Hsiao, M. C.; Yen, M. Y.; Chiou, K. C.; Lee, T. M. *Carbon* **2011**, *49*, 5107.
23. Park, S.; Ruoff, R. S. *Nat. Nanotechnol.* **2009**, *4*, 217.
24. Zhu, Y. W.; Murali, S.; Cai, W. W.; Li, X. S.; Suk, J. W.; Potts, J. R.; Ruoff, R. S. *Adv. Mater.* **2010**, *22*, 3906.
25. Dubin, S.; Gilje, S.; Wang, K.; Tung, V. C.; Cha, K.; Hall, A. S.; Farrar, J.; Varshneya, R.; Yang, Y.; Kaner, R. B. *ACS Nano* **2010**, *4*, 3845.
26. Paredes, J. I.; Villar-Rodil, S.; Fernández-Merino, M. J.; Guardia, L.; Martínez-Alonso, A.; Tascón, J. M. D. *J. Mater. Chem.* **2011**, *21*, 298.
27. Shervedani, R. K.; Amini, A. *Bioelectrochemistry* **2012**, *84*, 25.
28. Mocellini, S. K.; Fernandes, S. C.; Vieira, I. C. *Sens. Actuat. B* **2008**, *133*, 364.
29. Lee, H.; Dellatore, S. M.; Miller, W. M.; Messersmith, P. B. *Science* **2007**, *318*, 426.
30. Lee, H.; Lee, B. P.; Messersmith, P. B. *Nature* **2007**, *448*, 338.
31. Kaminska, I.; Das, M. R.; Coffinier, Y.; Niedziolka-Jonsson, J.; Sobczak, J.; Woisel, P.; Lyskawa, J.; Opallo, M.; Boukherroub, R.; Szunerits, S. *Appl. Mater. Interfaces* **2012**, *4*, 1016.
32. Hummers, W. S.; Offeman, R. E. *J. Am. Chem. Soc.* **1958**, *80*, 1339.
33. Chen, G. H.; Wu, D. J.; Weng, W. G.; Wu, C. L. *Carbon* **2003**, *41*, 579.
34. Bourlinos, A. B.; Gournis, D.; Petridis, D.; Szabó, T.; Szeri, A.; Dékány, I. *Langmuir* **2003**, *19*, 6050.
35. Stankovich, S.; Dikin, D. A.; Piner, R. D.; Kohlhaas, K. A.; Kleinhammes, A.; Jia, Y. Y.; Wu, Y.; Nguyen, S. T.; Ruoff, R. S. *Carbon* **2007**, *45*, 1558.
36. Lin, Z. Y.; Yao, Y. G.; Li, Z.; Liu, Y.; Li, Z.; Wong, C. P. *J. Phys. Chem. C* **2010**, *114*, 14819.
37. Fernández-Merino, M. J.; Guardia, L.; Paredes, J. I.; Villar-Rodil, S.; Solis-Fernandez, P.; Martínez-Alonso, A.; Tascón, J. M. D. *J. Phys. Chem. C* **2010**, *114*, 6426.
38. Park, S. J.; Lee, K. S.; Bozoklu, G.; Cai, W. W.; Nguyen, S. T.; Ruoff, R. S. *ACS Nano* **2008**, *2*, 572.
39. Fan, Z. J.; Kai, W.; Yan, J.; Wei, T.; Zhi, L. J.; Feng, J.; Ren, Y. M.; Song, L. P.; Wei, F. *ACS Nano* **2011**, *5*, 191.
40. Kuila, T.; Bose, S.; Khanra, P.; Mishra, A. K.; Kim, N. H.; Lee, J. H. *Carbon* **2012**, *50*, 914.
41. Shen, J. F.; Hu, Y. Z.; Li, C.; Qin, C.; Ye, M. X. *Small* **2009**, *5*, 82.
42. Becerril, H. A.; Mao, J.; Liu, Z.; Stoltenberg, R. M.; Bao, Z.; Chen, Y. *ACS Nano* **2008**, *2*, 463.
43. Kotov, N. A.; Dekany, I.; Fendler, J. H. *Adv. Mater.* **1996**, *8*, 637.
44. Abdalla, M.; Dean, D.; Robinson, P.; Nyairo, E. *Polymer* **2008**, *49*, 3310.
45. Shen, M.; He, J.; Cui, Y.; Xinxin. *J. Elastomers Plast.* **2010**, *42*, 499.
46. Omrani, A.; Simon, C. L.; Rostami, A. A. *Mater. Chem. Phys.* **2009**, *114*, 145.
47. Garrett, K. W.; Rosenberg, H. M. *J. Phys. D: Appl. Phys.* **1974**, *7*, 1247.
48. Dang, Z. M.; Wang, L.; Yin, Y.; Zhang, Q. *Adv. Mater.* **2007**, *19*, 852.
49. Huang, X. Y.; Jiang, P. K.; Xie, L. Y. *Appl. Phys. Lett.* **2009**, *95*, 242901.
50. Li, M.; Huang, X. Y.; Wu, C.; Xu, H. P.; Jiang, P. K.; Toshikatsu, T. *J. Mater. Chem.* **2012**, *22*, 23477.
51. Dang, Z. M.; Yao, S. H.; Yuan, J. K.; Bai, J. B. *J. Phys. Chem. C* **2010**, *114*, 13204.